Time-resolved measurement of the local lattice temperature in terahertz quantum cascade lasers

Miriam S. Vitiello,[1,a)] Gaetano Scamarcio,[1,b)] and Vincenzo Spagnolo[2]
[1]*CNR-INFM Regional Laboratory LIT*^{3} *and Dipartimento Interateneo di Fisica "M. Merlin," Università degli Studi di Bari, Via Amendola 173, 70126 Bari, Italy*
[2]*CNR-INFM Regional Laboratory LIT*^{3} *and Dipartimento Interateneo di Fisica "M. Merlin," Politecnico di Bari, Via Amendola 173, 70126 Bari, Italy*

(Received 8 January 2008; accepted 19 February 2008; published online 12 March 2008)

We measured the time dependence of the local lattice temperature in terahertz quantum cascade lasers with surface plasmon waveguides. The time constants for heat extraction from the active region (0.15–0.29 μs) are approximately ten times shorter than those associated with heat extraction from the substrate, thereby showing the dominant role of the substrate-heat sink coupling. Thermal diffusivities $D=0.052$ cm^2/s ($D_s=3.9$ cm^2/s) and thermal diffusion lengths $\mu=1.2$ μm ($\mu_s=31$ μm) in the active region (substrate) have been extracted by fitting the solution of the heat transport equation to the experimental data. © *2008 American Institute of Physics*.
[DOI: 10.1063/1.2894585]

To improve the temperature performance of terahertz quantum cascade lasers (QCLs)[1], it is mandatory to understand the heat diffusion in such a complex structure. In particular, knowledge of the heat diffusion transient dynamics will guide the design of active regions, waveguides, and mounting configurations, aiming at a better thermal coupling with the heat sink. The steady-state thermal properties of QCLs have been extensively studied both experimentally[2–4] and theoretically.[4–7] As per the transient properties, only preliminary results, for mid-IR QCLs, have been reported in literature.[8–11] However, the latter piece of information is still lacking for terahertz QCLs.

In this paper, we report on time-resolved photoluminescence (PL) experiments to measure the active region temperatures of terahertz QCLs in pulsed operation. This approach allows to quantify the efficacy of the heating and cooling processes both in the active region and the substrate. The investigated devices are based on a combination of bound-to-continuum active region and surface plasmon optical waveguides.[12,13] The wafer was processed in 150 μm wide, 2 mm long laser bars by conventional photolithography. A detailed description of device fabrication, electrical and optical characteristics are reported in Ref. 12. The lasers were indium bonded, substrate side, on copper holders, mounted on the cold head of a helium flow microcryostat, and kept at a fixed heat sink temperature $T_H=70$ K. The latter was controlled by means of a calibrated Si diode, mounted close to the device. The 647 nm line of a Kr^+ laser was focused directly onto the QCL front facet down to a spot of ~1.5 μm diameter by using an 80×80 times long-working-distance planoachromatic microscope objective lens. The sample position was varied using a two-dimensional translation stage with 0.1 μm spatial resolution. The PL signal was dispersed using a 0.64 m monochromator and detected with an intensified Si charge coupled device (ICCD) having a time resolution of 20 ns. The ICCD head was equipped with a digital delay generator having rise and fall times of 1 and 1.5 ns, respectively. The pulse gating with respect to an input trigger can be controlled within 1 ns. At frequencies in the range $f=20-40$ kHz, the readout noise ranges between four and six counts rms.

PL spectra have been collected following the experimental procedure described in Fig. 1. Pulse widths (PWs) in the range of 0.3–2 μs, at a constant frequency $f=40$ KHz have been used. The delay between the ICCD trigger and the current pulse is $t_d \sim 130$ ns [see Fig. 1(b)]. A reading gate of 30 ns was opened at regular time steps of 30 ns, both before, during, and after the applied voltage pulse to the QCL [Fig. 1(c)]. Representative PL spectra measured at times $t \leqslant t_d$, $t_d \leqslant t \leqslant t_d+\mathrm{PW}$ and $t_d+\mathrm{PW} \leqslant t \leqslant t_d+1/f$, are shown in Figs. 1(d)–1(f). The main peaks correspond to band-to-band transitions between the ground state levels in the injector miniband and valence subbands. In Figs. 1(d) and 1(f), no evidence of transitions coming from conduction subbands populated by the applied electric field are visible since at $t \leqslant t_d$ and $t_d+\mathrm{PW} \leqslant t \leqslant t_d+1/f$, no current flows in the device. In contrast, an additional structure on the high energy

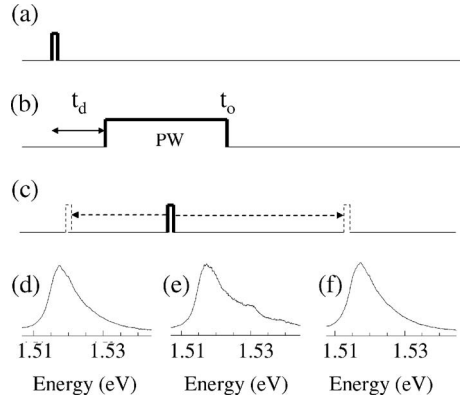

FIG. 1. Schematics of the time-resolved PL experiments. (a) ICCD trigger signal. (b) Voltage pulse delayed by the time t_d. (c) CCD gate opened before, during, and after the voltage pulse. [(d)–(f)] Representative PL spectra collected at a heat sink temperature $T_H=70$ K, with a time delay of (d) $t=30$ ns, (e) $t=1$ μs, and (f) $t=9$ μs. The QCL operated in pulsed mode with a frequency $f=40$ kHz, PW=1 μs, and an instantaneous electrical power $P=4$ W.

a)Electronic mail: vitiello@fisica.uniba.it.
b)Electronic mail: scamarcio@fisica.uniba.it.

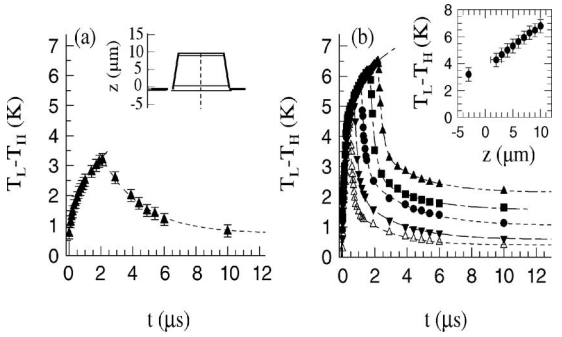

FIG. 2. (a) Difference between the lattice temperature T_L and the heat sink temperature T_H=70 K plotted as a function of time (t) in the substrate (z=−3 μm), in pulsed operation at f=40 kHz with a PW=2 μs, while an instantaneous electrical power P=4 W is applied to the device. The dashed lines at $t \leqslant 2$ μs and $t \geqslant 2$ μs are best solutions of the heat equation during and after the pulse, respectively. Inset: schematic of the investigated QCLs front facet. The dashed line indicates the locations along the device centre investigated by microprobe PL. (b) Difference between the lattice temperature T_L and the heat sink temperature T_H=70 K plotted as a function of time (t) close to the top of the active region (z=10 μm). The pulse frequency is f=40 kHz. The PWs are: PW=0.3 μs (bottom), 0.5 μs, 1 μs, 1.5 μs, and 2 μs (top) and an instantaneous electrical power P=4 W is applied to the device. The dashed lines are biexponential fits to the data. Inset: experimental temperature profile measured at a heat sink temperature T_H=70 K, along the Z axis in the device center, for the investigated QCL driven by an electrical power P=4 W at a duty cycle of 8%.

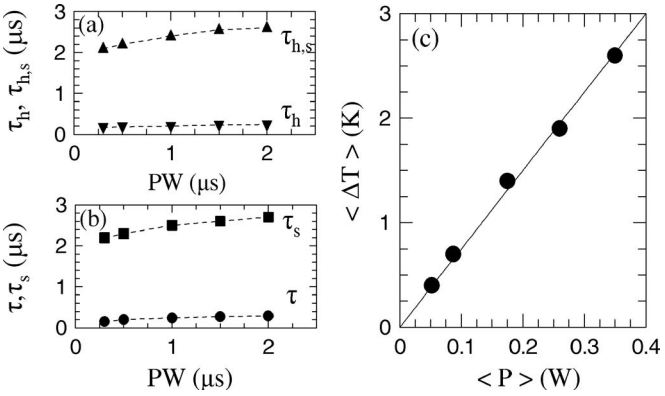

FIG. 3. (a) Heating thermal time constants τ_h (▼) and $\tau_{h,s}$ (▲), plotted as a function of the PW, as extracted from the biexponential fit shown in Fig. 2. (a) Cooling time constants τ (●) and τ_s (■), plotted as a function of the PW, as extracted from the biexponential fits of Fig. 2. The device operated at T_H=70 K in pulsed mode (f=40 kHz) with P=4 W. (c) Averaged difference between the lattice temperature T_L and the heat sink one, in the active region of the investigated device measured as a function of the mean electrical power. The experimental points correspond to device operation in pulsed mode with duty cycles equal to 1.2%, 2%, 4%, 6%, and 8%.

tail of the main band is visible in Fig. 1(e). This structure is associated with band-to-band transitions arising from the high energy conduction subbands populated by electron transport.[14,15] Also, the main band weakly redshifts with t due to the induced Joule heating effect under device operation. This shift can be used as a thermometric property to estimate the device local lattice temperature (T_L), following the experimental procedure described in Refs. 3 and 16.

Figure 2(a) shows the difference $\Delta T = T_L - T_H$ as a function of t, measured, in the GaAs substrate at z=−3 μm, by applying 2 μs long pulses. The time dependence of ΔT can be readily reproduced by solving the heat diffusion equation $\rho c(\partial T_L/\partial t) = \nabla(k \nabla T_L) + \dot{q}$, where ρ is the material density (g/cm^3), c is the specific heat capacity (J/g K), k is the thermal conductivity (W/cm K), and $\dot{q}$ is the energy density generation rate (W/cm^3). By using constant flux boundary conditions at the active region-substrate interface $q_0 = -k(dT_L/dz)$, considering that the heat source is localized in the active region and neglecting the longitudinal and lateral thermal gradients in proximity of the active region-substrate interface,[5,17] the resulting one-dimensional heat equation $\rho c(\partial T_L/\partial t) = k(\partial^2 T_L/\partial z^2)$ can be analytically solved. At $t \leqslant 2$ μs the solution is

$$\Delta T = T_{s,0} + \frac{q_0}{k}\left[2\sqrt{\frac{D_s t}{\pi}} e^{-z^2 D_s/4t} - z\left(1 - \mathrm{erf}\,\frac{z}{2\sqrt{D_s t}}\right)\right],$$

where D_s is the substrate thermal diffusivity and $T_{s,0}$ is the substrate temperature just before the pulse. At $t \geqslant 2$ μs, $\Delta T = T_{s,0} + T_s e^{-(t-t_0)/\tau_s}$, where t_0 is the time at the end of the pulse, τ_s is the thermal time constant associated with the cooling process from the substrate toward the heat sink, and T_s is the maximum temperature growth. From the analysis of the heating and cooling processes, we extracted D_s=3.9 cm^2/s (Ref 18) and τ_s=2.6 μs, respectively. The parameter D_s is directly related to the thermal diffusion length μ_s in the substrate via the relation $D_s = \mu_s^2/\tau_s$ (Ref. 19), from which we can extract μ_s=31 μm.

Figure 2(b) shows ΔT as a function of t, measured at different PWs, close to the top of the device active region (z=10 μm), where the maximum temperature increase occurs.[2] The use of the simple heat diffusion equation fails to reproduce the heating of the active region, thus, suggesting that a more complete model, e.g., including an additional heat source localized at the top Schottky barrier should be used. This theoretical approach is beyond the aim of the present work and will be discussed elsewhere. The analysis of the measured transients [Fig. 2(b)] shows that, for $t_d \leqslant t \leqslant t_d$+PW, ΔT is well approximated by the following expression: $\Delta T = T_0 + T_h(1 - e^{-t/\tau_h}) + T_{h,s}(1 - e^{-t/\tau_{h,s}})$, where T_0 is the lattice temperature in the active region just before the pulse; T_h and $T_{h,s}$ are constant temperatures to be determined; and τ_h and $\tau_{h,s}$ are the heating time constants.[20] The temperature rise is controlled by the τ_h component, while the slower heat transfer via the substrate, the In solder and submount/heat sink interface is determined by $\tau_{h,s}$. Similarly, at t_d+PW $\leqslant t \leqslant t_d + 1/f$, the decrease of ΔT with t can be described via the biexponential solution $\Delta T = T_0 + T' e^{-(t-t_0)/\tau} + T_s e^{-(t-t_0)/\tau_s}$, where T' is a constant temperature to be determined and τ and τ_s are cooling time constants.[11] The biexponential fits shown in Fig. 2(b) indicate that there are two distinct cooling phases in the terahertz QCLs associated with τ and τ_s. We can relate the parameter τ to the heat initially escaping from the active region and the time constant τ_s to the second stage of cooling in which the heat diffuses toward the heat sink through the substrate, as confirmed from the comparison with the τ_s value extracted from the data of Fig. 2(a).

In the inset of Fig. 2(b), we show the lattice temperature distribution inside the active region. The experimental temperature profile has been measured along the z axis at T_H=70 K, while the QCL is driven by P=4 W by setting a duty cycle of 8% and by opening the CCD gate at $t = t_0$. Our results show that T_L increases according to a second order polynomial function, in agreement with the analytic solution of the heat transport equation.[2]

The τ_h and $\tau_{h,s}$ (τ and τ_s) values are plotted in Fig. 3(a)

[Fig. 3(b)] as a function of PW. The data show that $\tau \approx \tau_h$ and always one order of magnitude lower than $\tau_s \approx \tau_{h,s}$. Our results demonstrate that the cooling and heating processes in the investigated terahertz QCLs are characterized by a first rapid dynamic, that accounts for ~75% of the whole decrease/increase of ΔT [see Fig. 2(b)] and a subsequent slower heat transfer caused by the surface plasmon waveguide geometry and the poor thermal coupling at the substrate-heat sink interface.

A quantitative prediction on the potential improvements induced by alternative waveguide/mounting geometries would require the development and testing of a thermal model on the temporal heat transfer dynamic in terahertz QCLs. The latter model is actually still lacking. However, at the present stage, we can predict that (i) the use of thinner active regions may lead to a significant reduction of τ, despite the decrease in the optical overlap factor;[21] (ii) the use of smoothed interfaces and the consequent reduction of the thermal boundary resistance[22] may increase significantly the active region thermal diffusivity, thus, reducing τ and τ_h; (iii) the use of a double metal optical waveguide may improve the whole heat dissipation in the device and, thus, reduce the thermal time constants as suggested by previous experiments,[3] which demonstrated that metal-metal interfaces assure normalized thermal resistances up to five times lower than those of surface plasmon terahertz QCLs; and (iv) the epilayer-down mounting may allow a significant reduction of the τ_s/τ ratio, as confirmed by theoretical calculations performed in mid-IR QCLs, where a decrease of a factor ~5 in the ratio τ_s/τ has been estimated for epilayer-side mounted devices.[11]

Finally, the results shown in Figs. 3(a) and 3(b) show that by increasing PW, τ, τ_s, τ_h, and $\tau_{h,s}$ also increase, thus, indicating deterioration in the heat transfer. This effect can be easily explained considering the dependence of the cross-plane thermal conductivity in the active region $k_\perp$ from T_L. Our previous experiments on GaAs-based QCLs demonstrated that in the lattice temperature range (80–200 K], $k_\perp$ decreases by 10%.[2]

From the measured thermal time constants, if the cross-plane thermal diffusivity $D=k_\perp/\rho c$ is known, we can determine the active region thermal diffusion length. By using the values $k_\perp \sim 0.05$ W/cm K (Ref. 2) and $\rho=5.29$ g/cm^3, $c=0.181$ J/g K calculated as the weighted averages of the densities and specific heats of the well and barrier materials,[23] respectively, we found $D=0.052$ cm^2/s, approximately one order of magnitude lower than that of the GaAs bulk material. At PW=2 μs, we measured a diffusion length $\mu=1.2$ μm.

Finally, in Fig. 3(c), we show the averaged temperature difference $\langle \Delta T \rangle = f\int_0^{1/f} T_L(t)dt$, plotted as a function of the mean electrical power $\langle P \rangle$. From the slope of $\langle \Delta T \rangle$ versus $\langle P \rangle$, we can extract a thermal resistance value $R_L=8.2$ K/W, similar to that measured during device operation in continuous wave.[12]

CNR-INFM LIT^3 acknowledges partial financial support from Regione Puglia, PE-056. We gratefully acknowledge useful discussions with M. Pellicoro, S. Stramaglia, L. Angelini, and C. Evans. V.S. acknowledges the II Faculty of Engineering of the Politecnico di Bari for partial financial support.

[1] B. S. Williams, S. Kumar, Q. Hu, and J. L. Reno, Opt. Express **13**, 3331 (2005).
[2] M. S. Vitiello, G. Scamarcio, and V. Spagnolo, "Temperature dependence of thermal conductivity and boundary resistance in THz quantum cascade lasers," IEEE J. Sel. Top. Quantum Electron. (in press).
[3] M. S. Vitiello, G. Scamarcio, V. Spagnolo, J. Alton, S. Barbieri, C. Worral, H. E. Beere, D. A. Ritchie, and C. Sirtori, Appl. Phys. Lett. **89**, 021111 (2006).
[4] C. Pflugl, M. Litzenberger, W. Schrenk, D. Pogany, E. Gornik, and G. Strasser, Appl. Phys. Lett. **82**, 1664 (2003).
[5] A. Lops, V. Spagnolo, and G. Scamarcio, J. Appl. Phys. **100**, 043109 (2006).
[6] C. Zhu, Y. Zhang, A. Li, and Z. Tian, J. Appl. Phys. **100**, 053105 (2006).
[7] S. S. Howard, L. Zhijun, D. Wasserman, A. J. Hoffman, T. S. Ko, and C. F. Gmachl, IEEE J. Sel. Top. Quantum Electron. **13**, 1054 (2007).
[8] R. L. Tober, J. Appl. Phys. **101**, 044507 (2007).
[9] A. J. Borak, C. C. Phillips, and C. Sirtori, Appl. Phys. Lett. **82**, 4020 (2003).
[10] C. Zhu, Y. G. Zhang, A. Z. Li, and Y. L. Zheng, Semicond. Sci. Technol. **20**, 563 (2005).
[11] C. A. Evans, V. D. Jovanovic, D. Indjin, Z. Ikonic, and P. Harrison, IEEE J. Quantum Electron. **42**, 859 (2006).
[12] M. S. Vitiello, G. Scamarcio, V. Spagnolo, S. S. Dhillon, and C. Sirtori, Appl. Phys. Lett. **90**, 191115 (2007).
[13] The structure was grown by molecular beam epitaxy by a commercial provider. The active region included 90 periods of GaAs/$Al_{0.15}Ga_{0.85}As$ heterostructures and is sandwiched between an upper GaAs contact layer (80 nm thick) and a lower surface plasmon GaAs layer (600 nm thick), doped at levels of $n=5\times10^{18}$ cm^{-3} and $n=2\times10^{18}$ cm^{-3}, respectively.
[14] M. S. Vitiello, G. Scamarcio, and V. Spagnolo, J. Nanophoton. **1**, 013514 (2007).
[15] M. S. Vitiello, G. Scamarcio, V. Spagnolo, T. Losco, R. P. Green, A. Tredicucci, H. E. Beere, and D. A. Ritchie, Appl. Phys. Lett. **88**, 241109 (2006).
[16] M. S. Vitiello, G. Scamarcio, V. Spagnolo, B. S. Williams, S. Kumar, Q. Hu, and J. L. Reno, Appl. Phys. Lett. **86**, 111115 (2005).
[17] G. Scamarcio, M. S. Vitiello, V. Spagnolo, S. Kumar, B. S. Williams, and Q. Hu, "Nanoscale heat transfer in quantum cascade lasers," Physica E (Amsterdam) (in press).
[18] From the calculated D_s value, we extracted a substrate thermal conductivity $k \sim 3.9$ K/W cm, close to the values reported for bulk GaAs n doped to $n \leqslant 10^{16}$ cm^{-3}.
[19] P. K. L. Chan, P. Pipe, Z. Mi, J. Yang, P. Bhattacharya, and D. Luerben, Appl. Phys. Lett. **89**, 011110 (2006).
[20] M. Ziegel, F. Weik, J. W. Tomm, T. Elsaesser, W. Nakwaski, R. Sarzala, D. Lorenzen, J. Meusel, and A. Kozlowska, Appl. Phys. Lett. **89**, 263506 (2006).
[21] Y. Chassagneux, J. Palomo, R. Colombelli, S. Barbieri, S. Dhillon, C. Sirtori, H. Beere, J. Alton, and D. Ritchie, Electron. Lett. **43**, 285 (2007).
[22] M. S. Vitiello, G. Scamarcio, V. Spagnolo, A. Lops, Q. Yang, C. Manz, W. Bronner, K. Köhler, and J. Wagner, Appl. Phys. Lett. **90**, 121109 (2007).
[23] J. J. S. Blakemore, J. Appl. Phys. **53**, R123 (1982).